



Distribution and Sources of Dissolved Black Carbon in Surface Waters of the Chukchi Sea, Bering Sea, and the North Pacific Ocean

Motohiro Nakane¹, Taku Ajioka^{2†} and Youhei Yamashita^{1,2*}

¹ Division of Earth System Science, Graduate School of Environmental Science, Hokkaido University, Sapporo, Japan,

² Faculty of Environmental Earth Science, Hokkaido University, Sapporo, Japan

OPEN ACCESS

Edited by:

Cristina Santin,
Swansea University, UK

Reviewed by:

Matthew William Jones,
University of Exeter, UK
Philippa Louise Ascough,
Scottish Universities Environmental
Research Centre, UK

*Correspondence:

Youhei Yamashita
yamashiy@ees.hokudai.ac.jp

† Present Address:

Taku Ajioka,
Geological Survey of Japan, National
Institute of Advanced Industrial
Science and Technology AIST,
Tsukuba, Japan

Specialty section:

This article was submitted to
Biogeoscience,
a section of the journal
Frontiers in Earth Science

Received: 09 March 2017

Accepted: 27 April 2017

Published: 16 May 2017

Citation:

Nakane M, Ajioka T and Yamashita Y
(2017) Distribution and Sources of
Dissolved Black Carbon in Surface
Waters of the Chukchi Sea, Bering
Sea, and the North Pacific Ocean.
Front. Earth Sci. 5:34.
doi: 10.3389/feart.2017.00034

Pyrogenic carbon, also called black carbon (BC), is an important component in the global carbon cycle. BC produced by biomass burning or fossil fuel combustion is transported to oceans by the atmosphere or rivers. However, environmental dynamics (i.e., major sources and sinks) of BC in marine environments have not been well-documented. In this study, dissolved BC (DBC) collected from surface waters of the Chukchi Sea, the Bering Sea, and the subarctic and subtropical North Pacific were analyzed using the benzene polycarboxylic acid (BPCA) method. The DBC concentration and the ratio of B5CA and B6CA to all BPCAs (an index of the DBC condensation degree) ranged from 4.8 to 15.5 $\mu\text{g-C L}^{-1}$ and from 0.20 to 0.43, respectively, in surface waters of the Chukchi/Bering Seas and the North Pacific Ocean. The concentration and condensation degree of DBC in the Chukchi/Bering Seas were higher and more variable than those in the subarctic and subtropical North Pacific, which implies that the major factors controlling DBC distribution were different in these marine provinces. In the Chukchi/Bering Seas, the DBC concentration was negatively correlated to salinity but positively correlated to chromophoric dissolved organic matter (CDOM) quantity and total dissolved lignin phenol concentration estimated by CDOM parameters. These correlations indicated that the possible major source of DBC in the Chukchi/Bering Seas was Arctic rivers. However, in the North Pacific, where riverine inputs are negligible for most sampling sites, DBC was possibly derived from the atmosphere. Although spectral slopes of CDOM at 275–295 nm (an index of the photodegradation degree of CDOM) differed widely between the subarctic and subtropical North Pacific, the concentration and condensation degrees of DBC were similar between the subarctic and subtropical North Pacific, which suggests that photodegradation was not the only major factor controlling DBC distribution. Therefore, DBC distributions of the North Pacific Ocean were considered to be mainly controlled by atmospheric deposition of BC and subsequent losses by photodegradation and adsorption onto sinking particles. This study implies that the main influence on DBC distribution in the open ocean and the coastal ocean are atmospheric deposition and fluvial inputs, respectively.

Keywords: pyrogenic carbon, dissolved black carbon, surface waters, Chukchi Sea, Bering Sea, North Pacific

INTRODUCTION

Pyrogenic carbon (PyC), including soot, char, black carbon, and biochar, is produced by incomplete combustion of organic matter by biomass burning or fossil fuel combustion (Masiello, 2004). The physical and chemical characteristics of PyC vary widely and depend on formation temperature (Hedges et al., 2000; Masiello, 2004). Less aromatic PyC (e.g., char) produced at lower temperature is considered to be biologically degradable (Bruun et al., 2008); however, PyC produced at higher temperature forms more condensed polyaromatic compounds (e.g., soot and elemental carbon) and is considered to be stable in reduced carbon pools for at least thousands of years (e.g., Masiello and Druffel, 1998). Although the values are largely variable and depend on quantification methods, PyC content has been determined to be <1–60% (Preston and Schmidt, 2006) and generally 5–15% (Hockaday et al., 2007) of soil organic carbon and 2–50% of sedimentary organic carbon (Kuhlbusch, 1998). Recently, Reisser et al. (2016) generated a soil PyC database and found that global PyC represents 13.7% of the SOC on average and can even be up to 60%. Therefore, PyC has been considered an important potentially slow-cycling refractory component of the global carbon cycle, although the magnitude of key pools and fluxes in the global cycle of PyC remain poorly constrained (Kuhlbusch, 1998; Bird et al., 2015; Santín et al., 2016).

Recent studies have revealed occurrences of PyC in the dissolved organic matter (DOM) fraction, and such dissolved PyC has often been defined as dissolved black carbon (DBC) in aquatic environments (e.g., Dittmar, 2008; Jaffé et al., 2013). Fourier transform ion cyclotron resonance mass spectrometry (FT-ICR-MS) identified condensed aromatic ring structures in the DOM from soil pore water (Hockaday et al., 2006) and riverine water (Kim et al., 2004), indicating that a part of PyC in soils becomes water soluble during degradation and that the soluble fraction of PyC (DBC) in soil pore waters is exported to rivers (Hockaday et al., 2006, 2007).

To determine factors controlling riverine DBC concentrations and fluxes, spatial and temporal distributions of riverine DBC have been clarified from watersheds to global scales using benzene polycarboxylic acid (BPCA) methods. The method quantifies BPCAs produced through the oxidation of polyaromatic compounds in PyC (Dittmar, 2008). Dittmar et al. (2012a) determined the seasonal/annual variation of riverine DBC from 1997 to 2008 in tropical Atlantic forest watersheds that were extensively burned from the 1850s to 1973. They found that DBC continues to be mobilized from a watershed every year in rainy seasons, although widespread forest burning ceased more than 20 years ago. From the highest DBC concentrations in the wet season to the lowest in the dry season for the same river, Marques et al. (2017) indicated the important role of hydrology in DBC dissolution and migration. A strong linear correlation between DBC concentration and dissolved organic carbon (DOC) concentration has generally been found in rivers regardless of differences in watershed size or type or climatic provinces (Dittmar et al., 2012a,b; Ding et al., 2013, 2014, 2015; Wagner et al., 2015). It has recently been estimated that DBC contributes to the ~10% of DOC in global rivers (Jaffé et al., 2013;

Stubbins et al., 2015). The riverine DBC is finally transported to oceans (Mannino and Harvey, 2004; Masiello and Louchouart, 2013; Huang et al., 2016), and the global flux was estimated to be 26.5 ± 1.8 million tons, which is of the same order of magnitude as the estimated range of the annual production of PyC from vegetation fires (Jaffé et al., 2013).

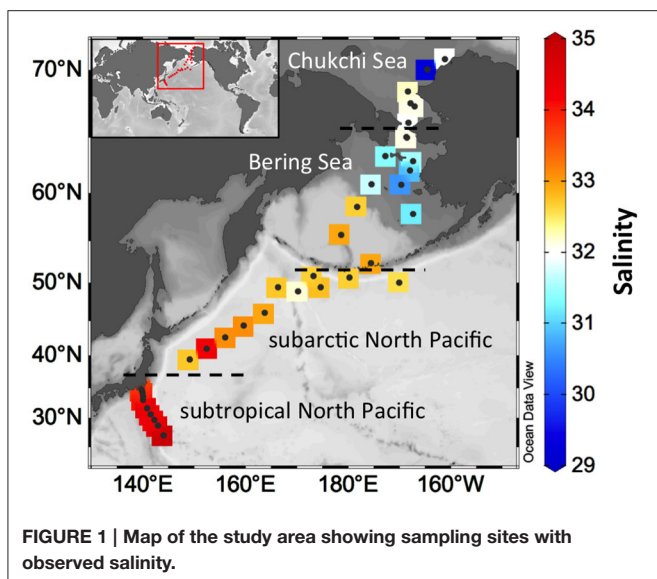
In marine environments, Dittmar and Koch (2006) used FT-ICR-MS and identified polyaromatic compounds with hydrophilic functional groups as DBC from DOM collected from the Southern Ocean. Using the BPCA method, the percentage of DBC in bulk marine DOM has been estimated to be 2.0–2.6% (Dittmar, 2008; Dittmar and Paeng, 2009; Coppola and Druffel, 2016), which is comparable to most chromatographically identifiable compounds (i.e., amino acids and neutral sugars) in marine DOM (Benner, 2002). Additionally, the apparent ^{14}C age of DBC was estimated to be 5,000–23,000 years (Ziolkowski and Druffel, 2010; Coppola and Druffel, 2016). These findings imply that DBC is likely a major fraction of refractory DOM in marine environments and is possibly important as a long-term carbon reservoir of the global carbon cycle.

Riverine and groundwater input (Dittmar et al., 2012a; Jaffé et al., 2013; Huang et al., 2016), atmospheric deposition (Jurado et al., 2008), and hydrothermal fluids (Dittmar and Koch, 2006; Dittmar and Paeng, 2009) have been proposed as possible sources of DBC in marine environments, whereas photodegradation (Stubbins et al., 2012) and adsorption onto sinking particles (Coppola et al., 2014) have been considered as potential sinks. However, because spatial and temporal distributions of DBC have scarcely been reported in marine environments (Dittmar and Paeng, 2009), the environmental dynamics (i.e., major sources and sinks) of marine DBC have not been well-documented, even in possible ranges of DBC concentration. Such knowledge is essential to evaluate not only the global PyC cycle but also the global carbon cycle. Therefore, distribution patterns of DBC in surface waters of the marginal seas (the Chukchi/Bering Seas) and the open ocean (the North Pacific Ocean) were determined in this study using the BPCA method to evaluate the range of DBC concentration and its controlling factors in the surface ocean. The major sources and possible loss processes are discussed from the geographical patterns of DBC, chromophoric DOM (CDOM), the UV, and visible light-absorbing constituent in DOM), and salinity.

MATERIALS AND METHODS

Sampling

Sampling locations with observed salinities are shown in **Figure 1**. Samplings of the Chukchi/Bering Seas and the subarctic North Pacific Ocean were carried out during two cruises in July 2013 by the T/S *Oshoro-Maru* (C255) and in July–August 2014 by the R/V *Hakuho Maru* (KH-14-3). Samplings of the subtropical North Pacific Ocean were carried out at 10 sites in July 2016 during the R/V *Shinsei Maru* cruise (KS-16-9). Surface water samples ($n = 38$) were collected using a towed fish metal-free sampling system (1–3 m below the surface, Tsumune et al., 2005; Nishioka et al., 2011) or an underway pumping system (~5 m



below the surface). Some samples ($n = 4$ at $70.7^{\circ}\text{N}/161.3^{\circ}\text{W}$, $70.1^{\circ}\text{N}/164.6^{\circ}\text{W}$, $67.7^{\circ}\text{N}/167.9^{\circ}\text{W}$, and $50.1^{\circ}\text{N}/170.1^{\circ}\text{W}$) were collected at 5–10 m using a conductivity-temperature-depth (CTD) system equipped with Niskin bottles. A deep seawater sample was also collected at 2,000 m at the subarctic western North Pacific Ocean in March 2015 during the R/V *Hakuhou Maru* KH-15-1 cruise. The deep seawater DOM sample was used to examine the BPCA method under nitric oxidation conditions as mentioned below.

Approximately 6–9 L of seawater was collected for DBC analysis. Seawater samples were filtered using a pre-combusted (450°C , 3–5 h) Whatman GF/F filter ($0.7\ \mu\text{m}$ of nominal pore size), and the filtrate was then poured into a 9-L acid-washed polycarbonate bottle. The polycarbonate bottle was covered with a black plastic bag to avoid photodegradation of DBC during sampling. Immediately after sampling, the filtrate pH was adjusted to 2 by HCl and the acidified filtrate was immediately subjected to solid phase extraction, as discussed in Section Solid Phase Extraction.

Samples for DOM optical analysis were filtered using a pre-combusted GF/F filter (KH-14-3 and KS-16-9 cruises) or an acid-washed $0.22\text{-}\mu\text{m}$ filter (C255 cruise). The filtered seawater was poured into a pre-combusted glass vial with a Teflon-lined cap after triple rinsing and then stored frozen (-20°C) in the dark until analysis.

Temperature was determined with CTD sensors during all the cruises. Salinity was also determined with a CTD sensor during the KS-16-9 cruise but was determined with a salinometer (AUTOSAL8400B, Guildline Instruments, Smiths Falls, ON, Canada) during the KH-14-3 and C255 cruises.

Solid Phase Extraction

A pre-concentration of DBC by solid phase extraction (SPE) was performed aboard a ship using the method of Dittmar (2008) with some modifications. The 6–9 L of acidified seawater

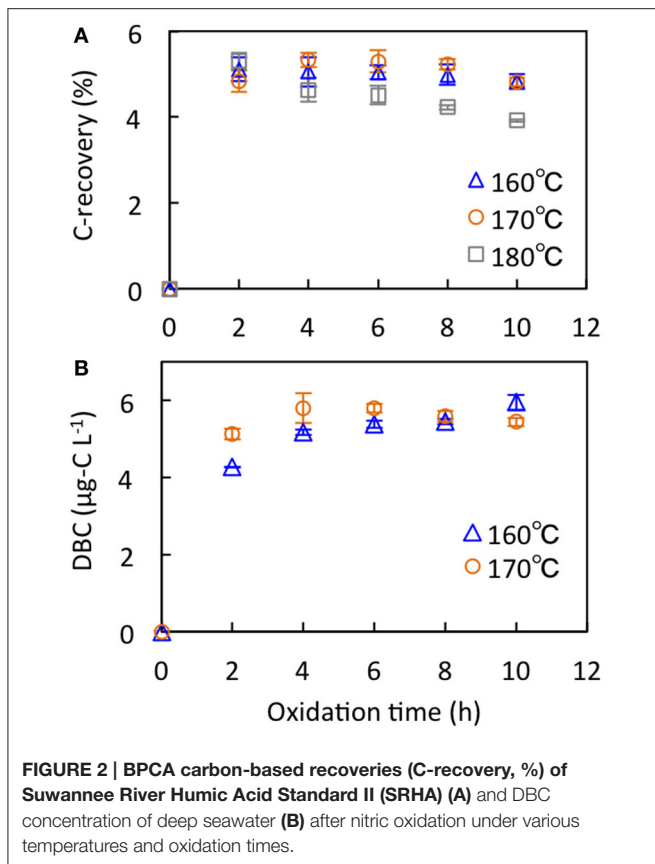
was passed through an SPE cartridge (1 g, Bond Elut PPL, Agilent Technologies) pre-conditioned by two column volumes of methanol. After the passage of acidified seawater, the cartridge was rinsed by two-column volumes of 0.01 M HCl, wrapped with aluminum foil, placed inside a plastic bag, and then stored frozen (-20°C) in the dark. In a laboratory on land, the frozen SPE cartridge was thawed and then dried under an N_2 stream. Two-column volumes of methanol were passed through the cartridge to elute the organic compounds, including DBC adsorbed on the cartridge resins. The eluate was poured into a glass vial with a Teflon-lined cap pre-cleaned by methanol and then stored frozen (-20°C) in the dark until DBC analysis by the BPCA method, as discussed in the following two sections.

Nitric Oxidation for the Benzene Polycarboxylic Acid (BPCA) Method

The BPCA method, a method for determining the molecular pyrogenic carbon, was originally employed for the quantification of PyC in soils (Glaser et al., 1998), but has been modified for a DBC analysis by Dittmar (2008). Polyaromatic compounds in PyC are oxidized to BPCAs by nitric acid, and the produced BPCAs are separated and can be quantified by using a high-performance liquid chromatograph coupled with a photodiode-array detector (HPLC-DAD), a gas chromatograph (GC) coupled with a flame ionization detector, or a GC coupled with mass spectrometer (e.g., Dittmar, 2008; Ziolkowski et al., 2011). BPCAs were not produced from non-thermogenic organic matter (Dittmar, 2008; Ding et al., 2013). In addition, the condensation degree, which may help to evaluate the source/processing of PyC, can also be obtained from the BPCA method (Glaser et al., 1998).

DBC analysis by the BPCA method was performed using the method of Dittmar (2008) and Ding et al. (2013). The eluate (3 ml) was transferred into a 2-ml glass ampoule over drying under an N_2 stream at room temperature; then, the ampoule was flame-sealed after the addition of 0.5 ml of concentrated HNO_3 . The sealed ampoule was kept in an oven at 170°C for 6 h. After the oxidation, HNO_3 was evaporated under an N_2 stream at 50°C , and samples in the ampoules were re-dissolved in 0.2 ml of mobile phase A (see details in the following section) for high-performance liquid chromatography (HPLC) analysis.

Different conditions have been reported for nitric oxidation for the BPCA method, e.g., 160°C for 6 h (Ding et al., 2013) or 170°C for 8 or 9 h (Glaser et al., 1998; Dittmar, 2008), and 180°C for 8 h (Ziolkowski et al., 2011). To compare the oxidation efficiencies under different conditions, the Suwannee River Humic Acid Standard II (SRHA, 2S101H) and the deep seawater DOM sample collected in this study were analyzed with various oxidation conditions of 160, 170, and 180°C for up to 10 h (Figure 2). The C-recovery of SRHA ranged from 3.9 to 5.3% (Figure 2A). Under oxidation at 160°C , there were no differences in C-recovery among the oxidation times (4.8–5.1%). The C-recoveries of oxidation times of 4–8 h (5.2–5.3%) were higher than those of 2 and 10 h (4.8%) at 170°C . The C-recovery under 180°C oxidation decreased with increasing oxidation time from 5.3% (2 h) to 3.9% (10 h). The oxidation at 170°C for 4–8 h showed the highest C-recovery of SRHA in



this study and showed slightly higher C-recovery compared with the highest value observed at 160°C for 6 h reported by Ding et al. (2013). The DBC concentration of deep seawater ranged from 4.2 to 6.0 µg-C L⁻¹ (Figure 2B). Under oxidation at 160°C, the DBC concentration increased with increasing oxidation time from 4.2 µg-C L⁻¹ (2 h) to 6.0 µg-C L⁻¹ (10 h), and the DBC concentration under 170°C oxidation for 4–6 h (5.7–5.8 µg-C L⁻¹) was higher than that for other times (5.1–5.6 µg-C L⁻¹). From these two experimental results, the oxidation at 170°C for 6 h was used as the condition of nitric oxidation for the BPCA method. Note that the C-recovery and DBC concentration at 170°C for 6 h were reproducible within ±5% for triplicate runs.

High Performance Liquid Chromatography to Quantify BPCAs

BPCAs were analyzed using an Agilent 1260 Infinity HPLC system equipped with a photodiode array detector (DAD; Dittmar, 2008). Briefly, samples/standards were eluted at a flow rate of 0.18 ml min⁻¹ following gradients from 94% mobile phase A (4 mM tetrabutylammonium bromide, 50 mM sodium acetate, and 10% MeOH) to 80% mobile phase B (MeOH) over 100 min with a C₁₈ column (3.5 µm, 2.1 × 150 mm, Waters Sunfire). A column oven of the HPLC system was set to 16°C. The quantification of the BPCAs was carried out with absorbance at 235 nm using the calibration curve of the BPCA standards mixture. The standards mixture of the BPCAs was prepared

with commercially available BPCAs (1,2,3-B3CA; 1,2,4-B3CA; 1,3,5-B3CA; 1,2,4,5-B4CA; B5CA; B6CA). Two commercially non-available BPCAs (1,2,3,4-B4CA and 1,2,3,5-B4CA) were identified by retention time and absorbance spectrum (220–380 nm; Dittmar, 2008). The quantification of these two BPCAs was performed using the calibration curve of 1,2,4,5-B4CA.

The DBC concentration was estimated from BPCA concentrations using an equation proposed by Dittmar (2008). The contribution (ratio) of B5CA and B6CA to total BPCAs was calculated as an index for condensation degree of DBC. The analytical error of the methods determined using triplicate seawater samples was <4% in terms of the DBC concentration.

Analysis of DOM Optical Properties

The absorbance spectrum between 200 and 800 nm was measured using a spectrophotometer (UV-1800, Shimadzu) with a 5-cm quartz windowed cell using the method of Yamashita et al. (2013). Briefly, water samples were thawed and allowed to stand prior to analysis until they reached room temperature (~23°C). Absorbance spectra of a blank (Milli-Q) and samples were obtained against air, and a blank spectrum was subtracted from each sample spectrum. The sample spectra were then baseline corrected by subtracting average values ranging from 590 to 600 nm from the entire spectrum (Yamashita and Tanoue, 2009). Absorbance was converted to the absorption coefficient $a(\lambda)$ (m⁻¹) and then fitted to an exponential function as follows (Green and Blough, 1994):

$$a(\lambda) = a(\lambda_i)e^{-S(\lambda-\lambda_i)},$$

where $a(\lambda)$ and $a(\lambda_i)$ are the absorption coefficients at wavelength λ and reference wavelength λ_i , respectively. S is the spectral slope parameter. In this study, the absorption coefficient at 254 nm (a_{254}) was reported as a quantitative parameter of CDOM. The S obtained between 275 and 295 nm ($S_{275-295}$) was calculated using the method of Helms et al. (2008). $S_{275-295}$ has been used as a proxy for the molecular weight of the DOM (e.g., Helms et al., 2008), a tracer for terrigenous DOM in coastal environments (Fichot et al., 2013; Fichot and Benner, 2014), and an index for the degree of photodegradation (e.g., Helms et al., 2008; Yamashita et al., 2013). In this study, the value of $S_{275-295}$ was used as indexes for the contribution of terrigenous DOM and the degree of photodegradation in the Chukchi/Bering Seas and the North Pacific Ocean. A smaller value of $S_{275-295}$ indicated a greater contribution of terrigenous DOM or a lower degree of photodegradation and *vice versa* (Fichot et al., 2013; Yamashita et al., 2013). Notably, the DBC determined by the BPCA method is one of the constituents of CDOM. However, although CDOM is a mixture of terrigenous organic matter such as lignin (e.g., Fichot et al., 2016), autochthonous humic-like materials (e.g., Yamashita and Tanoue, 2009), proteins (e.g., Yamashita and Tanoue, 2009), and so on, in addition to DBC, the contribution of DBC to CDOM remains poorly constrained. Thus, a_{254} and $S_{275-295}$ were used for indexes of bulk CDOM rather than DBC in this study.

Total dissolved lignin phenol concentration (TDLP₉, nM), a proxy for terrigenous DOM (Meyers-Schulte and Hedges, 1986; Opsahl and Benner, 1997; Fichot and Benner, 2012), was estimated using absorption coefficients and the equation proposed by Fichot et al. (2016). Note that the estimated TDLP₉ concentrations for samples in the open ocean most likely included some uncertainties because the equation was established with samples obtained from coastal environments while the autochthonous components possibly occupy major fractions of CDOM in the open ocean.

RESULTS

Oceanographic Characteristics of the Study Area

Temperature and salinity of surface waters observed in the Bering Sea showed relatively wide ranges, from 3.8 to 10.7°C (Supplemental Figure 1) and from 30.6 to 33.0 (Figure 1), respectively. The Bering Sea has a deep basin in the south and a shallow continental shelf in the northeast. The observed salinities in the shelf were lower than those in the basin. Levels of terrigenous CDOM are high in the shelf compared with the outer shelf (D'Sa et al., 2014). Temperature and salinity in the Chukchi Sea were lower than in the Bering Sea and ranged from -0.09 to 4.6°C and from 29.3 to 32.2, respectively. In the Bering-Chukchi shelf, several water masses, e.g., the Alaskan Coastal Water, the Bering Shelf Water, and the Anadyr Water, flow from the Bering Sea to the Chukchi Sea through the Bering Strait (Shimada et al., 2001; Grebmeier et al., 2006). The Alaskan Coastal Water, characterized by low salinity (Grebmeier et al., 2006), can be affected by riverine terrigenous DOM (Shin and Tanaka, 2004; Tanaka et al., 2016).

Sampling sites located between 39 and 51°N can be defined as within the subarctic North Pacific. In surface waters of the subarctic North Pacific, temperature and salinity were variable and ranged from 10.1 to 22.7°C and from 32.2 to 34.2, respectively. Sampling sites in this province were mainly located in the Western Subarctic Gyre (WSG), an area surrounded by the East Kamchatka, the Oyashio, and the Kuroshio currents. Some sites were located near the Aleutian Islands and are considered affected by the Alaskan Stream (Onishi and Ohtani, 1999).

In the subtropical region of the North Pacific (south of 35°N in this study), the temperature and salinity of surface waters ranged from 25.0 to 29.0°C and from 33.6 to 34.9, respectively. Sampling sites in this province were located at the western edge of the North Pacific Subtropical Gyre (NPSG); the sites covered the inside of the NPSG, the Kuroshio, and the outside of the NPSG. The Kuroshio water is characterized as warmer and more saline compared with the coastal water located at the outside of the NPSG (Kawabe and Yoneno, 1987). As shown in Supplemental Figure 2, five, two, and three sampling sites in the subtropical North Pacific were located at the inside of the NPSG, the Kuroshio, and the outside of the NPSG, respectively.

Spatial Distribution of DOM Optical Properties in Surface Waters

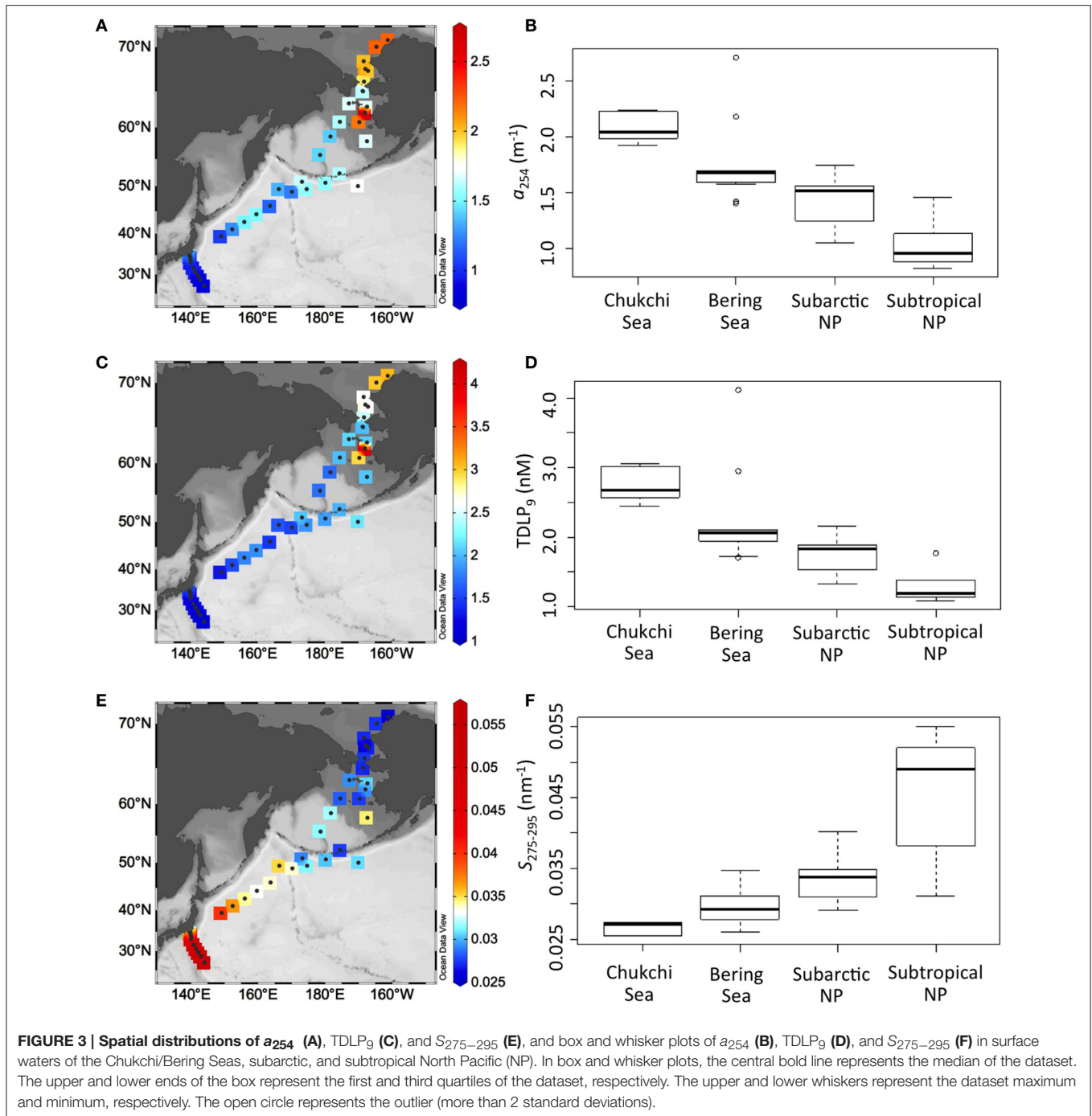
In the marginal seas, the levels of CDOM, expressed as a_{254} , were generally high in the Chukchi Sea (1.9–2.2 m⁻¹) compared with the Bering Sea (1.4–2.7 m⁻¹), although the highest level was observed at a site in the Bering Sea (Figures 3A,B). In the Bering Sea, levels of CDOM in the shelf were higher than those in the basin. The lowest level of CDOM was evident in surface waters of the subtropical North Pacific (0.8–1.5 m⁻¹); CDOM in surface waters of the subarctic North Pacific (1.1–1.7 m⁻¹) was in the middle range. Overall, the distribution pattern of CDOM levels in surface waters was similar to that of colored dissolved and detrital material (CDM) observed by ocean color imagery (Siegel et al., 2005) and that of humic-like fluorophores determined by excitation emission matrices combined with parallel factor analysis (Yamashita et al., 2017).

In analogy with the distribution pattern of a_{254} , the TDLP₉ concentration estimated from absorption coefficients was highest in the Chukchi Sea (2.4–3.1 nM), except for two samples obtained from the Bering Sea (3.0 and 4.1 nM), whereas the lowest values were observed in the subtropical North Pacific (1.1–1.8 nM; Figures 3C,D). Among the middle ranges of the TDLP₉ concentration, that of the Bering Sea (without two outliers, 1.7–2.1 nM) tended to be higher than that of the subarctic North Pacific (1.3–2.2 nM). Although the TDLP₉ concentration observed in the Chukchi Sea was within the range previously observed in the same region, the range of TDLP₉ observed in this study was extremely narrow compared with the range observed in various coastal environments (1–500 nM; Fichot et al., 2016).

$S_{275-295}$ was the lowest in the Chukchi Sea (0.025–0.027 nm⁻¹; Figures 3E,F). In the Bering Sea and the subarctic North Pacific, $S_{275-295}$ had middle values and ranged from 0.026 to 0.035 nm⁻¹ and from 0.029 to 0.040 nm⁻¹, respectively. In the subtropical North Pacific, $S_{275-295}$ had the highest value with greatest variability (0.031–0.055 nm⁻¹). Overall, the $S_{275-295}$ values observed in the Chukchi/Bering Seas were similar to previous observations in the same region (Dainard and Guéguen, 2013; D'Sa et al., 2014; Tanaka et al., 2016) but were higher than those in other Arctic margins, including the Eurasian Arctic Ocean, the Beaufort Sea, and the Gulf of Ob (Fichot et al., 2013). $S_{275-295}$ values observed in the subarctic and subtropical North Pacific were roughly the same as previously reported values in the western North Pacific (Yamashita et al., 2013).

Spatial Distribution of DBC Concentration and Composition in Surface Waters

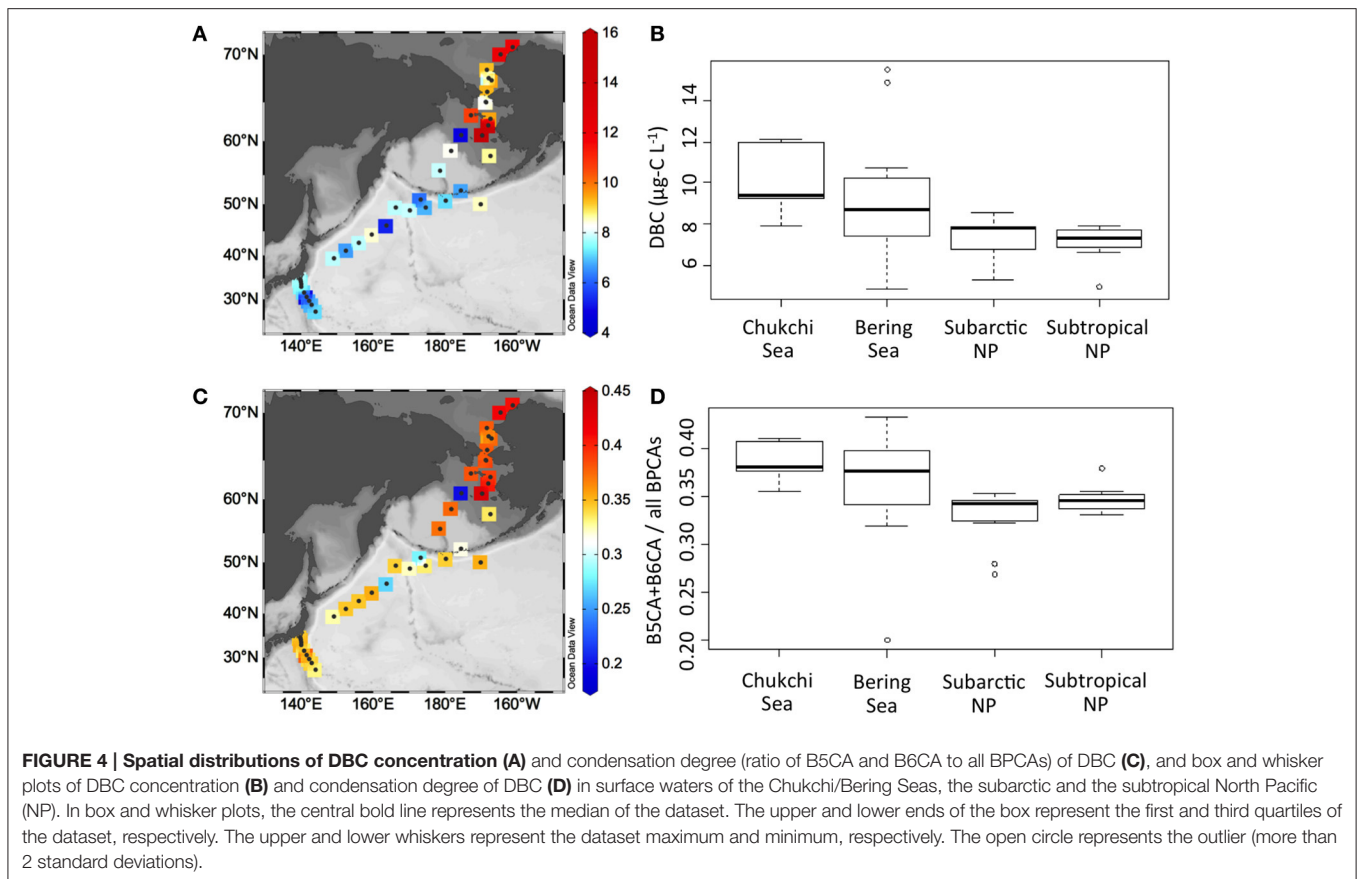
Figures 4A,B show spatial distributions and box and whisker plots of DBC concentration in surface waters of the Chukchi Sea, the Bering Sea, and the subarctic and subtropical North Pacific. Overall, DBC concentrations ranged from 4.8 to 15.5 μg-C L⁻¹ and were largely different among marine provinces. The DBC concentrations in the Chukchi Sea (7.9–12.1 μg-C L⁻¹) and the Bering Sea (4.8–15.5 μg-C L⁻¹) were higher than those in the subarctic and subtropical North Pacific (5.3–8.6 and 4.9–7.9 μg-C L⁻¹, respectively). In this study, the highest DBC concentrations were found at two sites in the shelf of the Bering



Sea. Because the DBC concentrations in the shelf were generally higher than those in the basin of the Bering Sea, the variability in the DBC concentration was greatest for the Bering Sea. DBC concentrations in the subarctic and subtropical North Pacific were within a narrow range and were similar to those in the basin of the Bering Sea.

Spatial distributions and box and whisker plots of the ratio of B5CA and B6CA to all BPCAs in surface waters of the Chukchi Sea, the Bering Sea, and the subarctic and subtropical North

Pacific are shown in **Figures 4C,D**. During nitric oxidation, highly substituted BPCAs (i.e., B6CA and B5CA) are formed from aromatic rings surrounded by many aromatic rings, whereas poorly substituted BPCAs (i.e., B3CA) are formed from aromatic rings surrounded by a few aromatic rings (Ziolkowski et al., 2011). Therefore, the ratio of B5CA and B6CA to all BPCAs can be used as an index for condensation degree of DBC. Overall, the ratio of B5CA and B6CA to all BPCAs ranged from 0.20 to 0.43 and showed systematic differences among marine provinces



(Figures 4C,D). The ratio was high in the Chukchi Sea (0.36–0.41) and Bering Sea (0.20–0.43) compared with the subarctic and subtropical North Pacific (0.27–0.35 and 0.33–0.38, respectively). In analogy with DBC concentration, the ratio in the Bering Sea was highly variable because of large differences between the shelf and the basin regions. The variability of the ratio in the subarctic and subtropical North Pacific was smaller than in the Chukchi/Bering Seas.

DISCUSSION

Characteristics of DBC in Surface Waters of the Chukchi Sea, Bering Sea, and North Pacific Ocean

DBC concentrations observed in this study were higher in the Chukchi/Bering Seas compared with the North Pacific Ocean (Figures 4A,B). The range of salinity (Figure 1), TDLP₉ (Figures 3C,D), and $S_{275-295}$ (Figures 3E,F) indicated that the study area at the Chukchi/Bering Seas received some riverine inputs. Previous studies reported DBC concentrations in riverine and marine DOM using the BPCA method with the same conversion method from BPCA to DBC concentration. Overall, the range of DBC concentration in marine environments observed in this study is one to three orders of magnitude lower than those observed in terrestrial aquatic environments (e.g., Jaffé et al., 2013; Stubbins et al., 2015), which indicates

that DBC in surface waters of coastal as well as oceanic environments is possibly derived from terrestrial environments by riverine inputs and/or atmospheric deposition, as previously reported (Dittmar, 2008; Dittmar and Paeng, 2009). The DBC concentrations in the Chukchi/Bering Seas (4.8–15.5 $\mu\text{g-C L}^{-1}$) were similar to a value reported for the open Gulf of Mexico (14.4 $\mu\text{g-C L}^{-1}$; Dittmar, 2008), and the DBC concentration in the North Pacific Ocean (4.9–8.6 $\mu\text{g-C L}^{-1}$) was slightly lower than those observed in the Southern Ocean (7.2–9.6 $\mu\text{g-C L}^{-1}$; Dittmar and Paeng, 2009) and in the North Atlantic Deep Water ($12.5 \pm 1.9 \mu\text{g-C L}^{-1}$; Stubbins et al., 2012).

The condensation degree of DBC was higher in marginal seas, i.e., the Chukchi/Bering Seas, compared with the open ocean, i.e., the subarctic and subtropical North Pacific (Figures 4C,D). Higher condensation degrees of DBC in coastal environments compared with the open ocean have also been reported (Dittmar, 2008; Dittmar and Paeng, 2009; Ziolkowski and Druffel, 2010). Interestingly, higher DBC concentration was generally accompanied by higher condensation degree of DBC, and *vice versa* throughout the study area (Figure 4). However, concentration and condensation degree of DBC were more variable in the Chukchi/Bering Seas compared with the North Pacific Ocean. Such a difference in variability possibly reflects different environmental dynamics (source and/or sink) of DBC between marginal seas and the open ocean.

Factors Controlling DBC Distributions in Surface Waters of the Chukchi/Bering Seas

DBC concentration was negatively correlated with salinity but was positively correlated with a_{254} and TDLP₉ in the surface waters of the Chukchi/Bering Seas (Figure 5). It has been recently reported that a_{254} is strongly correlated with DBC concentration in Arctic rivers (Stubbins et al., 2015). TDLP₉ has been used as a proxy of terrigenous DOM (Meyers-Schulte and Hedges, 1986; Opsahl and Benner, 1997; Fichot and Benner, 2012). Therefore, relationships between DBC and salinity, a_{254} , and TDLP₉ indicate that a major source of DBC in surface waters of the Chukchi/Bering Seas is riverine input. Rivers carry a large amount of DBC to global oceans, including the Arctic region (Jaffé et al., 2013; Stubbins et al., 2015). The correlation coefficient between DBC and salinity was lower than between DBC and a_{254} as well as TDLP₉ (Figure 5). The DOC concentration was not correlated to salinity in the Chukchi/Bering Seas because of the complex mixing of water masses, including sea-ice melt water, which can be characterized by low DOC concentration (Shin and Tanaka, 2004; Mathis et al., 2005; Tanaka et al., 2016). Therefore, it can be expected that the contribution of DBC in the sea-ice melt water disturbs the relationship between DBC and salinity in surface waters.

The plots were highly scattered between DBC concentration and $S_{275-295}$ (Figure 5D). Fichot and Benner (2012) noted that CDOM quality expressed as $S_{275-295}$ is photochemically altered in surface waters of salinities >30, regardless of origin. Several water masses, e.g., Alaskan Coastal Water (salinity < 31.8), Anadyr Water (salinity > 32.5), Bering Shelf Water (31.8–32.5 of salinity), have been known to distribute in the Chukchi/Bering Seas as marine end-members (Grebmeier et al., 2006). Therefore, scattered plots between DBC concentration and $S_{275-295}$ suggest the various degrees of photochemical degradation of DBC as well as CDOM among water masses of marine end-members.

The DBC concentration of the Yukon River in summer was $430 \mu\text{g-C L}^{-1}$ (Stubbins et al., 2015). This value is higher than the intercept ($69.7 \pm 19.3 \mu\text{g-C L}^{-1}$) of the linear regression between DBC concentration and salinity (Figure 5A). DBC concentrations in the glacier-fed and glacier-influenced rivers have been lower than those in rivers draining Alaskan boreal forest (Ding et al., 2015). Therefore, a part of the large difference in DBC concentration between the Yukon River (Stubbins et al., 2015) and the intercept (Figure 5A) is possibly a result of variable DBC concentrations among Arctic rivers, although sea-ice melt water should also contribute to the differences discussed above.

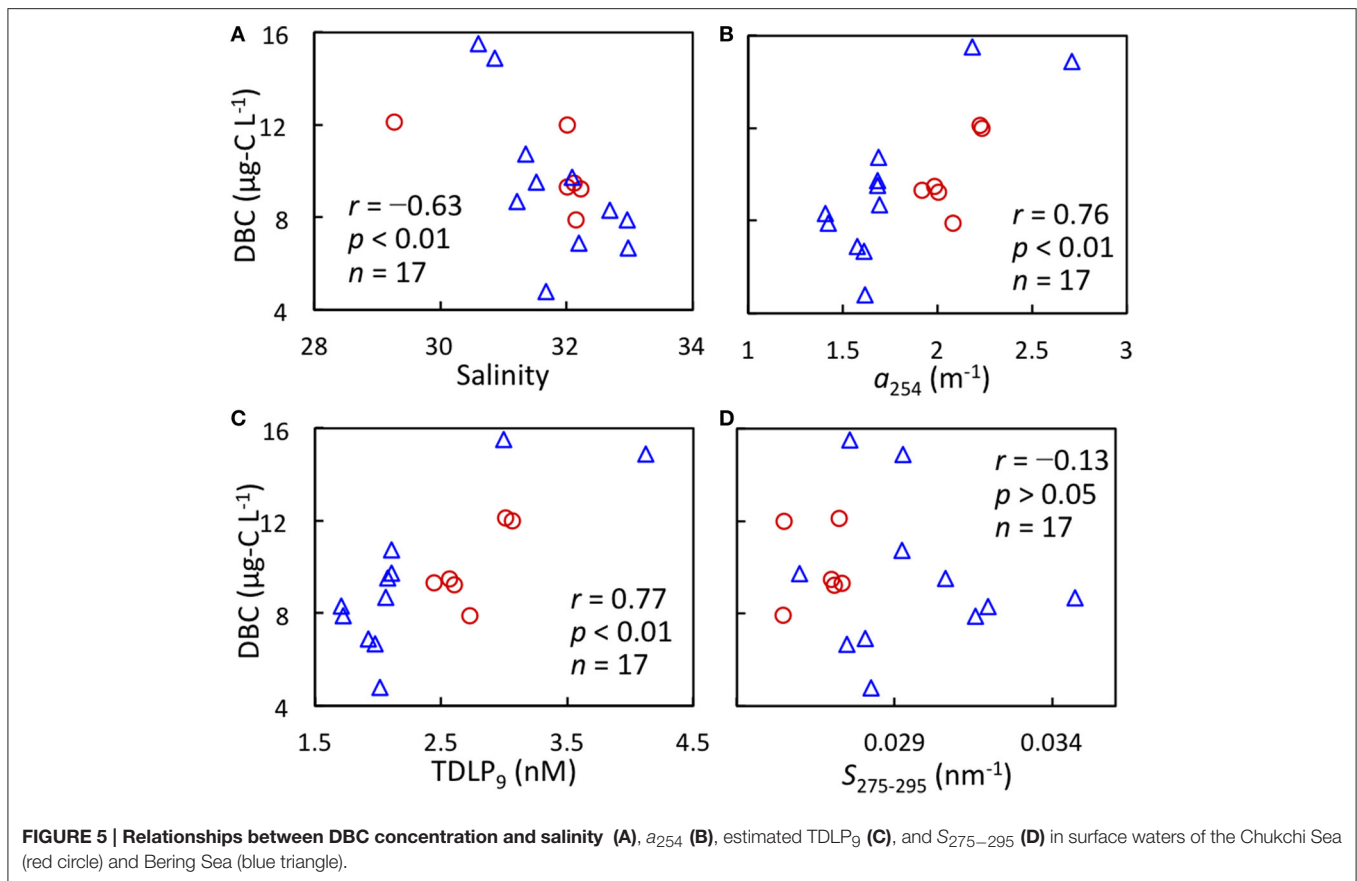
Factors Controlling DBC Distributions in Surface Waters of the North Pacific Ocean

DBC in surface waters of the North Pacific Ocean was characterized as having relatively low concentration and condensation (Figure 4). Because condensation degree of DBC becomes lower with photodegradation (Stubbins et al., 2010, 2012; Ward et al., 2014; Wagner and Jaffé, 2015; Fu et al., 2016), the relatively low concentration and condensation degree of DBC found in the North Pacific Ocean may result from extensive photodegradation. A large difference in $S_{275-295}$

was evident between the subarctic and subtropical North Pacific (Figures 3E,F). Because $S_{275-295}$ becomes larger with photodegradation of CDOM in the open ocean (Helms et al., 2008; Yamashita et al., 2013), the difference in $S_{275-295}$ suggests that the degree of photodegradation of CDOM (including DBC) was largely different between the subarctic and subtropical North Pacific. However, the DBC concentration and condensation degree were similar between the subarctic and subtropical North Pacific (Figure 4), which implies that photodegradation is not the sole major factor determining concentration and condensation degree of DBC in surface waters of the North Pacific Ocean. The other factor shaping the concentration and condensation degree of DBC in surface waters is adsorption onto sinking particles. Coppola et al. (2014) suggested that the transfer of hydrophobic, highly aromatic/condensed BC from DOC to particles is one of the important loss processes of DBC. The annual average flux of sinking particles from surface waters (at 60 and 100 m) to beneath the subarctic western North Pacific was similar or slightly higher than that in the subtropical western North Pacific (Honda et al., 2016). Thus, the similar ranges of the DBC concentration and condensation degree between the subarctic and subtropical North Pacific implies that the adsorption onto sinking particles is one of the processes shaping the DBC distribution in surface waters of the open ocean.

Atmospheric PyC (i.e., soot), produced during combustion at high temperature, such as fossil fuel combustion, can be characterized by a high condensation degree, and its oxidation products (BPCAs) are rich in B6CA and B5CA (Ziolkowski and Druffel, 2010; Roth et al., 2012). Therefore, we considered that the condensation degree of DBC derived from atmospheric deposition of PyC would be high. However, Ding et al. (2015) have recently reported that water soluble organic carbon extracted from atmospheric dust was rich in B3CA and B4CA and suggested that riverine DBC, which was rich in B3CA and B4CA, was the result of soot deposited onto the watersheds. Additionally, Khan et al. (2016) observed BPCA composition in recent freshwaters and ancient brines of perennially ice-covered, closed-basin Antarctic lakes and noted that the condensation degree of DBC derived from PyC of fossil fuel combustion was lower than that derived from wildfires. It has been well-recognized that soot particles in the atmosphere are rendered hydrophilic with chemical and photochemical aging (e.g., Petters et al., 2006; Weitkamp et al., 2007; Han et al., 2012). Thus, DBC with a low condensation degree is possibly derived from aged soot.

Salinity and $S_{275-295}$ (a_{254} and TDLP₉) in surface waters of the North Pacific Ocean were higher (lower) than those of the Chukchi/Bering Seas (Figures 1, 3), which implies that riverine inputs are minor in the North Pacific Ocean compared with those in the Chukchi/Bering Seas. Although the air-sea gas exchange fluxes of polycyclic aromatic hydrocarbons (PAHs) are high in the Arctic region, the PyC concentrations in aerosol particles and dry deposition of particle-bound PAHs in the North Pacific Ocean were greater than those in the Chukchi/Bering Seas (Hadley et al., 2007; Ma et al., 2013; Taketani et al., 2016). Low condensation degrees of DBC observed in surface waters of the subarctic and subtropical



North Pacific thus imply that atmospheric deposition of BC and subsequent dissolution is an important source of DBC in these provinces.

Distributional patterns of DBC concentration and condensation in the subtropical North Pacific support this conclusion. The sampling sites located at the outside of the NPSG may exhibit greater influence of riverine water compared with the sites located at the Kuroshio and the inside of the NPSG (Supplemental Figure 2). If major sources of DBC were riverine inputs in the subtropical North Pacific, there would be large gradients of DBC concentration and condensation from the outside to the inside of the NPSG. However, gradients of DBC concentration and condensation were not evident from the outside to the inside of the NPSG, although salinities in the outside of the NPSG were lower than those in the Kuroshio Current and the inside of the NPSG (Figure 6). These spatial distributions indicate that atmospheric deposition rather than riverine input is an important source of DBC in the surface waters of the North Pacific Ocean.

In summary, the relatively low concentration and condensation degree of DBC in the surface waters of the North Pacific Ocean are mainly because of atmospheric deposition of BC, with substantial effects of photodegradation and adsorption onto sinking particles.

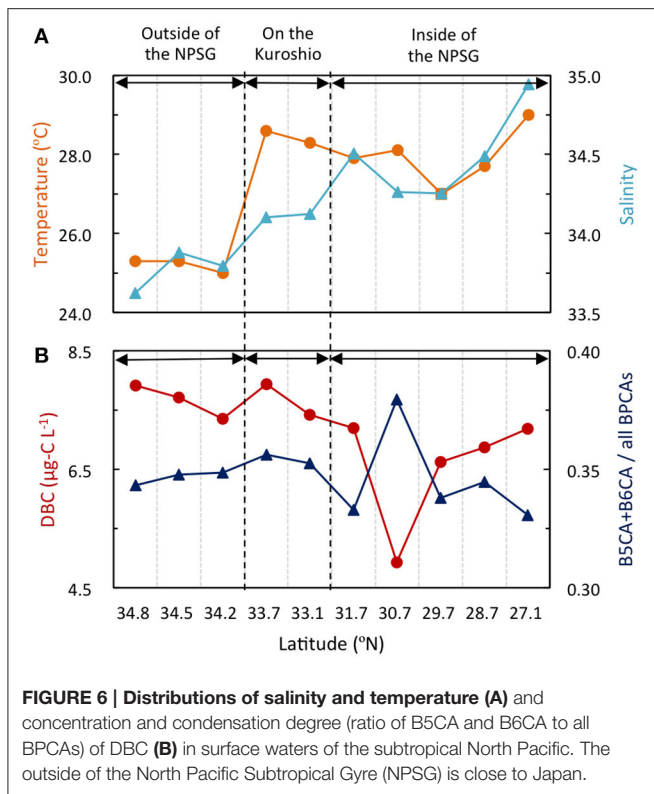
CONCLUSIONS AND REMARKS

DBC in the ocean is one of the important PyC pools on the Earth's surface. However, because ranges in DBC concentration and factors controlling DBC distribution have scarcely been reported, the environmental dynamics of marine DBC have not been well-documented. This study provides important insights about the environmental dynamics of DBC in surface waters of marginal seas and the open ocean.

The riverine input of DBC as a major source affects the distribution of DBC in the surface waters of the Chukchi/Bering Seas, in addition to possible contributions of DBC from sea-ice melt water, photodegradation of DBC in marine end-members, and variable DBC concentration among Arctic rivers.

The atmospheric deposition of BC and subsequent losses by photodegradation and adsorption onto sinking particles are the major factors shaping the relatively low concentration and condensation degree of DBC in the surface waters of the North Pacific Ocean.

This study indicates that the major sources of DBC in the open ocean and coastal ocean are atmospheric deposition and fluvial inputs, respectively. For the major loss processes of DBC in surface waters, photodegradation and adsorption onto sinking particles are considered. However, since atmospheric deposition, photodegradation, and adsorption onto sinking particles affect DBC distribution, all of which lower the condensation degree



and adsorption onto sinking particles. The evaluation of the DBC concentration in sea-ice melt water, various riverine waters, including glacier-fed and glacier-influenced water, and marine end-members are also necessary to clarify the factors shaping DBC distribution in the Arctic Ocean, including the Chukchi/Bering Seas.

AUTHOR CONTRIBUTIONS

MN and YY contributed to the design of the study. YY collected samples, performed SPE, and analyzed CDOM. MN performed BPCA analyses and data analyses with the help of TA and YY. MN wrote the initial draft of the manuscript, and all authors contributed to its revision.

ACKNOWLEDGMENTS

We are grateful to H. Ogawa, J. Nishioka, T. Hirawake, and the captains and crews of the R/V *Hakuho Maru*, the R/V *Shinsei Maru*, and the T/S *Oshoro-Maru* for their assistance with sample collection. We also thank the reviewers and guest editor, Dr. Santín, for their helpful and constructive comments and suggestions, which have improved the quality of this manuscript. This study was financially supported by the Grants-in-Aid (No. 16H0293006 and 24121003) from Japan Society for the Promotion of Science (JSPS) to YY.

SUPPLEMENTARY MATERIAL

The Supplementary Material for this article can be found online at: <http://journal.frontiersin.org/article/10.3389/feart.2017.00034/full#supplementary-material>

of DBC, the possible contributions of these processes could not be separated by the DBC proxy applied in this study (i.e., the ratio of B5CA and B6CA to total BPCAs). A new compositional proxy of DBC is needed to separately evaluate the effect of atmospheric deposition, photodegradation,

REFERENCES

- Benner, R. (2002). "Chemical composition and reactivity," in *Biogeochemistry of Marine Dissolved Organic Matter*, eds D. A. Hansell and C. A. Carlson (San Diego, CA: Academic Press), 59–90.
- Bird, M. I., Wynn, J. G., Saiz, G., Wurster, C. M., and McBeath, A. (2015). The pyrogenic carbon cycle. *Annu. Rev. Earth Planet. Sci.* 43, 273–298. doi: 10.1146/annurev-earth-060614-105038
- Bruun, S., Jensen, E. S., and Jensen, L. S. (2008). Microbial mineralization and assimilation of black carbon: dependency on degree of thermal alteration. *Organ. Geochem.* 39, 839–845. doi: 10.1016/j.orggeochem.2008.04.020
- Coppola, A. I., and Druffel, E. R. M. (2016). Cycling of black carbon in the ocean. *Geophys. Res. Lett.* 43, 4477–4482. doi: 10.1002/2016GL068574
- Coppola, A. I., Ziolkowski, L. A., Masiello, C. A., and Druffel, E. R. M. (2014). Aged black carbon in marine sediments and sinking particles. *Geophys. Res. Lett.* 41, 2427–2433. doi: 10.1002/2013GL059068
- Dainard, P. G., and Guéguen, C. (2013). Distribution of PARAFAC modeled CDOM components in the North Pacific Ocean, Bering, Chukchi and Beaufort seas. *Mar. Chem.* 157, 216–223. doi: 10.1016/j.marchem.2013.10.007
- Ding, Y., Cawley, K. M., Da Cunha, C. N., and Jaffé, R. (2014). Environmental dynamics of dissolved black carbon in wetlands. *Biogeochemistry* 119, 259–273. doi: 10.1007/s10533-014-9964-3
- Ding, Y., Yamashita, Y., Dodds, W. K., and Jaffé, R. (2013). Dissolved black carbon in grassland streams: is there an effect of recent fire history? *Chemosphere* 90, 2557–2562. doi: 10.1016/j.chemosphere.2012.10.098
- Ding, Y., Yamashita, Y., Jones, J., and Jaffé, R. (2015). Dissolved black carbon in boreal forest and glacial rivers of central Alaska: assessment of biomass burning versus anthropogenic sources. *Biogeochemistry* 123, 15–25. doi: 10.1007/s10533-014-0050-7
- Dittmar, T. (2008). The molecular level determination of black carbon in marine dissolved organic matter. *Organ. Geochem.* 39, 396–407. doi: 10.1016/j.orggeochem.2008.01.015
- Dittmar, T., De Rezende, C. E., Manecki, M., Niggemann, J., Ovalle, A. R. C., Stubbins, A., et al. (2012a). Continuous flux of dissolved black carbon from a vanished tropical forest biome. *Nat. Geosci.* 5, 618–622. doi: 10.1038/ngeo1541
- Dittmar, T., and Koch, B. P. (2006). Thermogenic organic matter dissolved in the abyssal ocean. *Mar. Chem.* 102, 208–217. doi: 10.1016/j.marchem.2006.04.003
- Dittmar, T., and Paeng, J. (2009). A heat-induced molecular signature in marine dissolved organic matter. *Nat. Geosci.* 2, 175–179. doi: 10.1038/ngeo440
- Dittmar, T., Paeng, J., Gihring, T. M., Suryaputra, I. G. N. A., and Huettel, M. (2012b). Discharge of dissolved black carbon from a fire-affected intertidal system. *Limnol. Oceanogr.* 57:1171. doi: 10.4319/lo.2012.57.4.1171
- D'Sa, E. J., Goes, J. L., Gomes, H., and Mouw, C. (2014). Absorption and fluorescence properties of chromophoric dissolved organic matter of the eastern Bering Sea in the summer with special reference to the influence of a cold pool. *Biogeosciences* 11, 3225–3244. doi: 10.5194/bg-11-3225-2014

- Ficht, C. G., and Benner, R. (2012). The spectral slope coefficient of chromophoric dissolved organic matter (S275-295) as a tracer of terrigenous dissolved organic carbon in river-influenced ocean margins. *Limnol. Oceanogr.* 57, 1453–1466. doi: 10.4319/lo.2012.57.5.1453
- Ficht, C. G., and Benner, R. (2014). The fate of terrigenous dissolved organic carbon in a river-influenced ocean margin. *Global Biogeochem. Cycles* 28, 300–318. doi: 10.1002/2013GB004670
- Ficht, C. G., Benner, R., Kaiser, K., Shen, Y., Amon, R. M., Ogawa, H., et al. (2016). Predicting dissolved lignin phenol concentrations in the coastal ocean from chromophoric dissolved organic matter (CDOM) absorption coefficients. *Front. Mar. Sci.* 3:7. doi: 10.3389/fmars.2016.00007
- Ficht, C. G., Kaiser, K., Hooker, S. B., Amon, R. M., Babin, M., Bélanger, S., et al. (2013). Pan-Arctic distributions of continental runoff in the Arctic Ocean. *Sci. Rep.* 3:1053. doi: 10.1038/srep01053
- Fu, H., Liu, H., Mao, J., Chu, W., Li, Q., Alvarez, P. J. J., et al. (2016). Photochemistry of dissolved black carbon released from biochar: reactive oxygen species generation and phototransformation. *Environ. Sci. Technol.* 50, 1218–1226. doi: 10.1021/acs.est.5b04314
- Glaser, B., Haumaier, L., Guggenberger, G., and Zech, W. (1998). Black carbon in soils: the use of benzenecarboxylic acids as specific markers. *Organ. Geochem.* 29, 811–819. doi: 10.1016/S0146-6380(98)00194-6
- Grebmeier, J. M., Cooper, L. W., Feder, H. M., and Sirenko, B. I. (2006). Ecosystem dynamics of the Pacific-influenced northern Bering and Chukchi Seas in the Amerasian Arctic. *Prog. Oceanogr.* 71, 331–361. doi: 10.1016/j.pocean.2006.10.001
- Green, S. A., and Blough, N. V. (1994). Optical absorption and fluorescence properties of chromophoric dissolved organic matter in natural waters. *Limnol. Oceanogr.* 39, 1903–1916. doi: 10.4319/lo.1994.39.8.1903
- Hadley, O. L., Ramanathan, V., Carmichael, G. R., Tang, Y., Corrigan, C. E., Roberts, G. C., et al. (2007). Trans-Pacific transport of black carbon and fine aerosols ($D < 2.5 \mu\text{m}$) into North America. *J. Geophys. Res. Atmos.* 112:D05309. doi: 10.1029/2006JD007632
- Han, C., Liu, Y., Ma, J., and He, H. (2012). Key role of organic carbon in the sunlight-enhanced atmospheric aging of soot by O₂. *Proc. Natl. Acad. Sci. U.S.A.* 109, 21250–21255. doi: 10.1073/pnas.1212690110
- Hedges, J. I., Eglinton, G., Hatcher, P. G., Kirchman, D. L., Arnosti, C., Derenne, S., et al. (2000). The molecularly-uncharacterized component of nonliving organic matter in natural environments. *Organ. Geochem.* 31, 945–958. doi: 10.1016/S0146-6380(00)00096-6
- Helms, J. R., Stubbins, A., Ritchie, J. D., Minor, E. C., Kieber, D. J., and Mopper, K. (2008). Absorption spectral slopes and slope ratios as indicators of molecular weight, source, and photobleaching of chromophoric dissolved organic matter. *Limnol. Oceanogr.* 53, 955–969. doi: 10.4319/lo.2008.53.3.0955
- Hockaday, W. C., Grannas, A. M., Kim, S., and Hatcher, P. G. (2006). Direct molecular evidence for the degradation and mobility of black carbon in soils from ultrahigh-resolution mass spectral analysis of dissolved organic matter from a fire-impacted forest soil. *Organ. Geochem.* 37, 501–510. doi: 10.1016/j.orggeochem.2005.11.003
- Hockaday, W. C., Grannas, A. M., Kim, S., and Hatcher, P. G. (2007). The transformation and mobility of charcoal in a fire-impacted watershed. *Geochim. Cosmochim. Acta* 71, 3432–3445. doi: 10.1016/j.gca.2007.02.023
- Honda, M. C., Kawakami, H., Matsumoto, K., Wakita, M., Fujiki, T., Mino, Y., et al. (2016). Comparison of sinking particles in the upper 200 m between subarctic station K2 and subtropical station S1 based on drifting sediment trap experiments. *J. Oceanogr.* 72, 373–386. doi: 10.1007/s10872-015-0280-x
- Huang, G., Chen, Y., Tian, C., Tang, J., Zhang, H., Luo, Y. M., et al. (2016). Spatial distributions and seasonal variations of dissolved black carbon in the Bohai Sea, China. *J. Coast. Res.* 74, 214–227. doi: 10.2112/SI74-019.1
- Jaffé, R., Ding, Y., Niggemann, J., Vähätalo, A. V., Stubbins, A., Spencer, R. G. M., et al. (2013). Global charcoal mobilization from soils via dissolution and riverine transport to the oceans. *Science* 340, 345–347. doi: 10.1126/science.1231476
- Jurado, E., Dachs, J., Duarte, C. M., and Simo, R. (2008). Atmospheric deposition of organic and black carbon to the global oceans. *Atmos. Environ.* 42, 7931–7939. doi: 10.1016/j.atmosenv.2008.07.029
- Kawabe, M., and Yoneno, M. (1987). Water and flow variations in Sagami Bay under the influence of the Kuroshio path. *J. Oceanogr. Soc. Japan* 43, 283–294. doi: 10.1007/BF02108696
- Khan, A. L., Jaffé, R., Ding, Y., and McKnight, D. M. (2016). Dissolved black carbon in Antarctic lakes: chemical signatures of past and present sources. *Geophys. Res. Lett.* 43, 5750–5757. doi: 10.1002/2016GL068609
- Kim, S., Kaplan, L. A., Benner, R., and Hatcher, P. G. (2004). Hydrogen-deficient molecules in natural riverine water samples—evidence for the existence of black carbon in DOM. *Mar. Chem.* 92, 225–234. doi: 10.1016/j.marchem.2004.06.042
- Kuhlbusch, T. A. (1998). Black carbon and the carbon cycle. *Science* 280, 1903–1904. doi: 10.1126/science.280.5371.1903
- Ma, Y., Xie, Z., Yang, H., Möller, A., Halsall, C., Cai, M., et al. (2013). Deposition of polycyclic aromatic hydrocarbons in the North Pacific and the Arctic. *J. Geophys. Res. Atmos.* 118, 5822–5829. doi: 10.1002/jgrd.50473
- Mannino, A., and Harvey, H. R. (2004). Black carbon in estuarine and coastal ocean dissolved organic matter. *Limnol. Oceanogr.* 49, 735–740. doi: 10.4319/lo.2004.49.3.0735
- Marques, J. S. J., Dittmar, T., Niggemann, J., Almeida, M. G., Gomez-Saez, G. V., and Rezende, C. E. (2017). Dissolved black carbon in the headwaters-to-ocean continuum of Paraíba Do Sul River, Brazil. *Front. Earth Sci.* 5:11. doi: 10.3389/feart.2017.00011
- Masiello, C. A. (2004). New directions in black carbon organic geochemistry. *Mar. Chem.* 92, 201–213. doi: 10.1016/j.marchem.2004.06.043
- Masiello, C. A., and Druffel, E. R. M. (1998). Black carbon in deep-sea sediments. *Science* 280, 1911–1913. doi: 10.1126/science.280.5371.1911
- Masiello, C. A., and Louchouart, P. (2013). Fire in the ocean. *Science* 340, 287–288. doi: 10.1126/science.1237688
- Mathis, J. T., Hansell, D. A., and Bates, N. R. (2005). Strong hydrographic controls on spatial and seasonal variability of dissolved organic carbon in the Chukchi Sea. *Deep Sea Res. Part II Top. Stud. Oceanogr.* 52, 3245–3258. doi: 10.1016/j.dsr2.2005.10.002
- Meyers-Schulte, K. J., and Hedges, J. I. (1986). Molecular evidence for a terrestrial component of organic matter dissolved in ocean water. *Nature* 321, 61–63. doi: 10.1038/321061a0
- Nishioka, J., Ono, T., Saito, H., Sakaoka, K., and Yoshimura, T. (2011). Oceanic iron supply mechanisms which support the spring diatom bloom in the Oyashio region, western subarctic Pacific. *J. Geophys. Res. Oceans* 116:C02021. doi: 10.1029/2010JC006321
- Onishi, H., and Ohtani, K. (1999). On seasonal and year to year variation in flow of the Alaskan Stream in the central North Pacific. *J. Oceanogr.* 55, 597–608. doi: 10.1023/A:1007840802296
- Opsahl, S., and Benner, R. (1997). Distribution and cycling of terrigenous dissolved organic matter in the ocean. *Nature* 386, 480–482. doi: 10.1038/386480a0
- Petters, M. D., Prenni, A. J., Kreidenweis, S. M., DeMott, P. J., Matsunaga, A., Lim, Y. B., et al. (2006). Chemical aging and the hydrophobic-to-hydrophilic conversion of carbonaceous aerosol. *Geophys. Res. Lett.* 33:L24806. doi: 10.1029/2006GL027249
- Preston, C. M., and Schmidt, M. W. I. (2006). Black (pyrogenic) carbon in boreal forests: a synthesis of current knowledge and uncertainties. *Biogeosciences* 3, 397–420. doi: 10.5194/bg-3-397-2006
- Reisser, M., Purves, R. S., Schmidt, M. W. I., and Abiven, S. (2016). Pyrogenic carbon in soils: a literature-based inventory and a global estimation of its content in soil organic carbon and stocks. *Front. Earth Sci.* 4:80. doi: 10.3389/feart.2016.00080
- Roth, P. J., Lehdorff, E., Brodowski, S., Bornemann, L., Sanchez-García, L., Gustafsson, Ö., et al. (2012). Differentiation of charcoal, soot and diagenetic carbon in soil: method comparison and perspectives. *Organ. Geochem.* 46, 66–75. doi: 10.1016/j.orggeochem.2012.01.012
- Santín, C., Doerr, S. H., Kane, E. S., Masiello, C. A., Ohlson, M., Rosa, J. M., et al. (2016). Towards a global assessment of pyrogenic carbon from vegetation fires. *Glob. Chang. Biol.* 22, 76–91. doi: 10.1111/gcb.12985
- Shimada, K., Carmack, E. C., Hatakeyama, K., and Takizawa, T. (2001). Varieties of shallow temperature maximum waters in the western Canadian Basin of the Arctic Ocean. *Geophys. Res. Lett.* 28, 3441–3444. doi: 10.1029/2001GL013168
- Shin, K. H., and Tanaka, N. (2004). Distribution of dissolved organic matter in the eastern Bering Sea, Chukchi Sea (Barrow Canyon) and Beaufort Sea. *Geophys. Res. Lett.* 31:L24304. doi: 10.1029/2004gl021039
- Siegel, D. A., Maritorena, S., Nelson, N. B., and Behrenfeld, M. J. (2005). Independence and interdependencies among global ocean color properties: Reassessing the bio-optical assumption. *J. Geophys. Res. Oceans* 110:C07011. doi: 10.1029/2004JC002527

- Stubbins, A., Niggemann, J., and Dittmar, T. (2012). Photo-lability of deep ocean dissolved black carbon. *Biogeosciences* 9, 1661–1670. doi: 10.5194/bg-9-1661-2012
- Stubbins, A., Spencer, R. G. M., Chen, H., Hatcher, P. G., Mopper, K., Hernes, P. J., et al. (2010). Illuminated darkness: molecular signatures of Congo River dissolved organic matter and its photochemical alteration as revealed by ultrahigh precision mass spectrometry. *Limnol. Oceanogr.* 55, 1467–1477. doi: 10.4319/lo.2010.55.4.1467
- Stubbins, A., Spencer, R. G. M., Mann, P. J., Holmes, R. M., McClelland, J. W., Niggemann, J., et al. (2015). Utilizing colored dissolved organic matter to derive dissolved black carbon export by arctic rivers. *Front. Earth Sci.* 3:63. doi: 10.3389/feart.2015.00063
- Taketani, F., Miyakawa, T., Takashima, H., Komazaki, Y., Pan, X., Kanaya, Y., et al. (2016). Shipborne observations of atmospheric black carbon aerosol particles over the Arctic Ocean, Bering Sea, and North Pacific Ocean during September 2014. *J. Geophys. Res. Atmos.* 121, 1914–1921. doi: 10.1002/2015JD023648
- Tanaka, K., Takesue, N., Nishioka, J., Kondo, Y., Ooki, A., Kuma, K., et al. (2016). The conservative behavior of dissolved organic carbon in surface waters of the southern Chukchi Sea, Arctic Ocean, during early summer. *Sci. Rep.* 6:34123. doi: 10.1038/srep34123
- Tsumune, D., Nishioka, J., Shimamoto, A., Takeda, S., and Tsuda, A. (2005). Physical behavior of the SEEDS iron-fertilized patch by sulphur hexafluoride tracer release. *Prog. Oceanogr.* 64, 111–127. doi: 10.1016/j.pocean.2005.02.018
- Wagner, S., Cawley, K. M., Rosario-Ortiz, F. L., and Jaffé, R. (2015). In-stream sources and links between particulate and dissolved black carbon following a wildfire. *Biogeochemistry* 124, 145–161. doi: 10.1007/s10533-015-0088-1
- Wagner, S., and Jaffé, R. (2015). Effect of photodegradation on molecular size distribution and quality of dissolved black carbon. *Organ. Geochem.* 86, 1–4. doi: 10.1016/j.orggeochem.2015.05.005
- Ward, C. P., Sleighter, R. L., Hatcher, P. G., and Cory, R. M. (2014). Insights into the complete and partial photooxidation of black carbon in surface waters. *Environ. Sci. Process. Impacts* 16, 721–731. doi: 10.1039/C3EM00597F
- Weitkamp, E. A., Sage, A. M., Pierce, J. R., Donahue, N. M., and Robinson, A. L. (2007). Organic aerosol formation from photochemical oxidation of diesel exhaust in a smog chamber. *Environ. Sci. Technol.* 41, 6969–6975. doi: 10.1021/es070193r
- Yamashita, Y., Hashihama, F., Saito, H., Fukuda, H., and Ogawa, H. (2017). Factors controlling the geographical distribution of fluorescent dissolved organic matter in the surface waters of the Pacific Ocean. *Limnol. Oceanogr.* doi: 10.1002/lno.10570. [Epub ahead of print].
- Yamashita, Y., Nosaka, Y., Suzuki, K., Ogawa, H., Takahashi, K., and Saito, H. (2013). Photobleaching as a factor controlling spectral characteristics of chromophoric dissolved organic matter in open ocean. *Biogeosciences* 10, 7207–7217. doi: 10.5194/bg-10-7207-2013
- Yamashita, Y., and Tanoue, E. (2009). Basin scale distribution of chromophoric dissolved organic matter in the Pacific Ocean. *Limnol. Oceanogr.* 54, 598–609. doi: 10.4319/lo.2009.54.2.0598
- Ziolkowski, L. A., Chamberlin, A. R., Greaves, J., and Druffel, E. R. M. (2011). Quantification of black carbon in marine systems using the benzene polycarboxylic acid method: a mechanistic and yield study. *Limnol. Oceanogr. Methods* 9, 140–149. doi: 10.4319/lom.2011.9.140
- Ziolkowski, L. A., and Druffel, E. R. M. (2010). Aged black carbon identified in marine dissolved organic carbon. *Geophys. Res. Lett.* 37:L16601. doi: 10.1029/2010GL043963

Conflict of Interest Statement: The authors declare that the research was conducted in the absence of any commercial or financial relationships that could be construed as a potential conflict of interest.

Copyright © 2017 Nakane, Ajioka and Yamashita. This is an open-access article distributed under the terms of the Creative Commons Attribution License (CC BY). The use, distribution or reproduction in other forums is permitted, provided the original author(s) or licensor are credited and that the original publication in this journal is cited, in accordance with accepted academic practice. No use, distribution or reproduction is permitted which does not comply with these terms.